伽马暴X射线偏振观测技术

刘倩

代表CXPD 合作组

中国科学院大学

高能宇宙线物理及下一代空间探测装置研讨会 2025 乌鲁木齐

汇报内容

contents

一、空间X射线偏振观测

二、POLAR-2/LPD

三、LPD飞行样机CXPD立方星

空间X射线偏振

- X射线偏振的产生与高能粒子在磁场中的非热辐射、辐射的非对称散射以及辐射在转移过程中的各向异性散射等物理过程相关；
- X射线的偏振起源于辐射源的**几何结构、辐射机制、磁场位形**等；

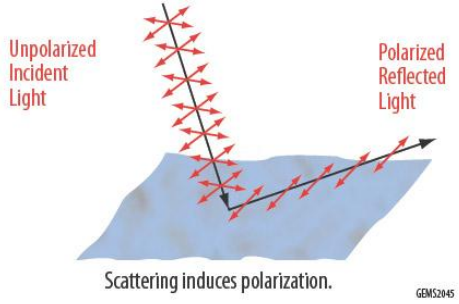

非偏的X射线经天体表面散射，产生偏振X射线

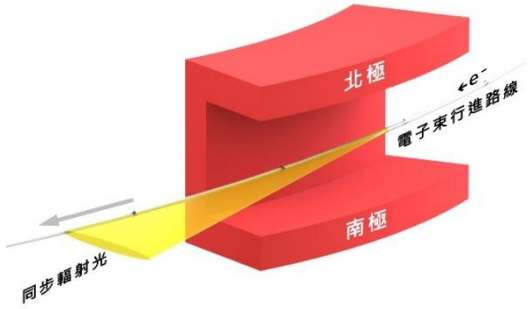

同步辐射产生的X射线具有明显的偏振特性

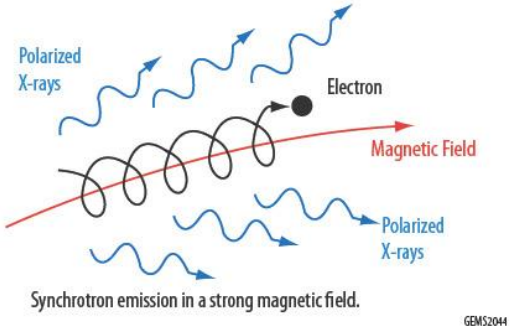

电子在强磁场环境下辐射出偏振X射线

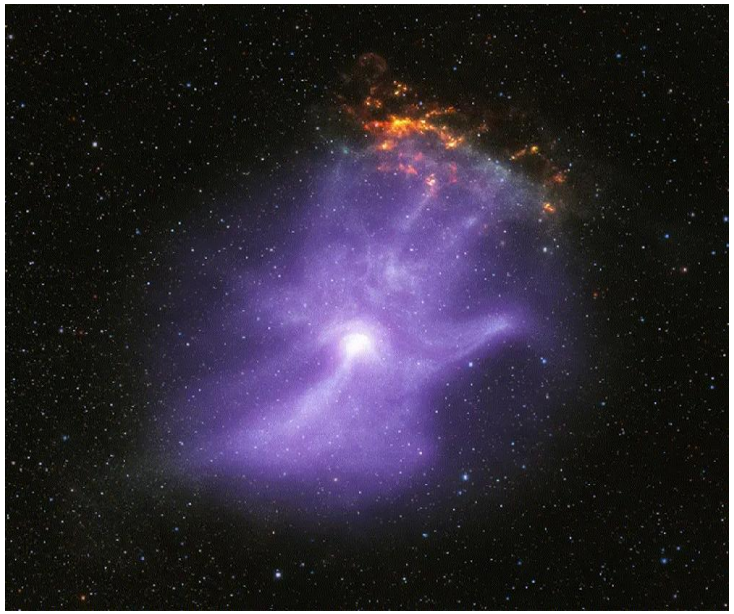

用偏振信号窥视不可见的磁场！

X射线偏振观测的发展历程

1968
散射偏振仪
探空火箭 Aerobee 150

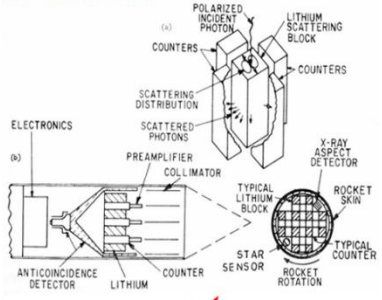

1971
布拉格偏振仪
探空火箭 Aerobee 350

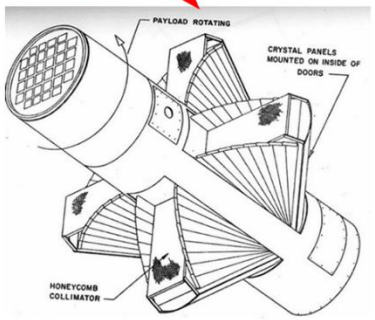

1974
平板布拉格偏振仪
卫星 Ariel 5

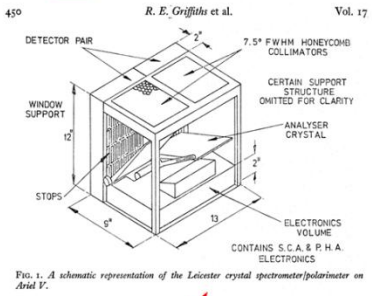

Fig. 1. A schematic representation of the Leicester crystal spectrometer/polarimeter on Ariel V.

1975
布拉格偏振仪
卫星 OSO-8

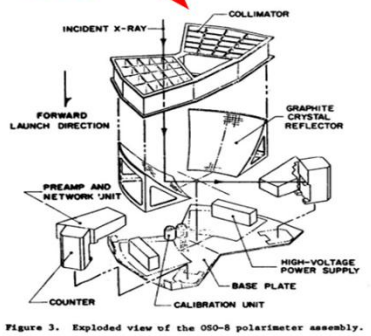

Figure 3. Exploded view of the OSO-8 polarimeter assembly.

2001
光电效应偏振仪
气体像素探测器 GPD

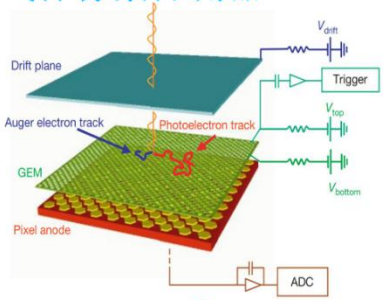

2018
光电效应偏振仪 GPD
立方星 PolarLight

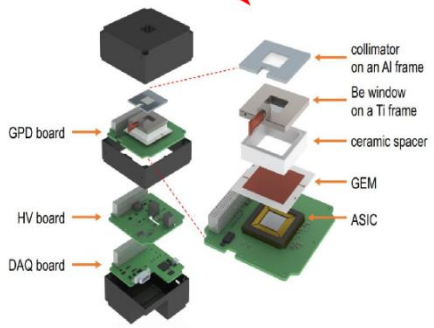

2021
光电效应偏振仪 GPD
卫星 IXPE

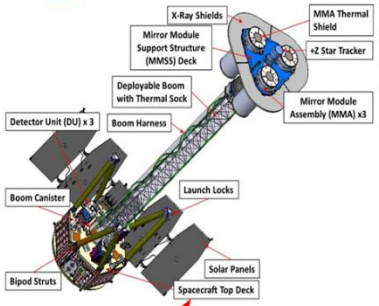

2023
光电效应偏振仪 GMPD
立方星 **CXPD01**
技术验证

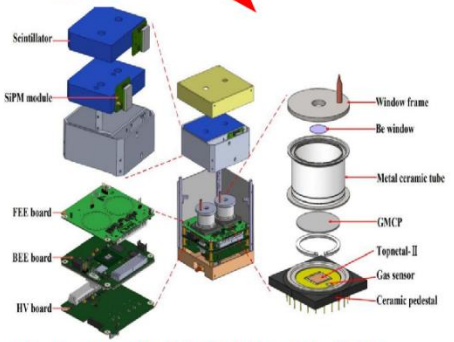

2025
光电效应偏振仪 GMPD
立方星 **CXPD02**
宽视场巡天

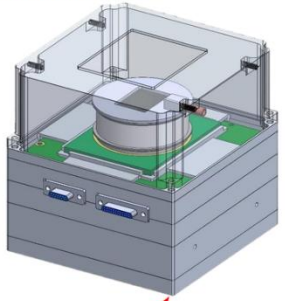

2025
光电效应偏振仪 GMPD
立方星 **CXPD03/04**
多星协同观测

GRB X射线偏振

伽马射线暴——恒星爆炸或致密天体并合

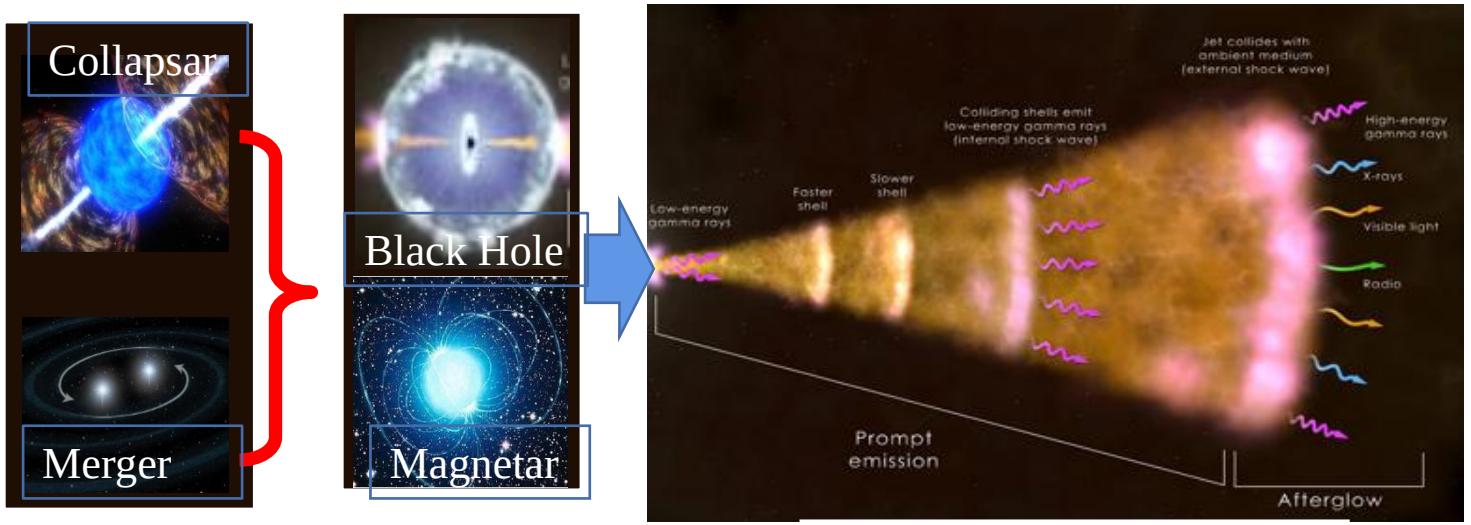

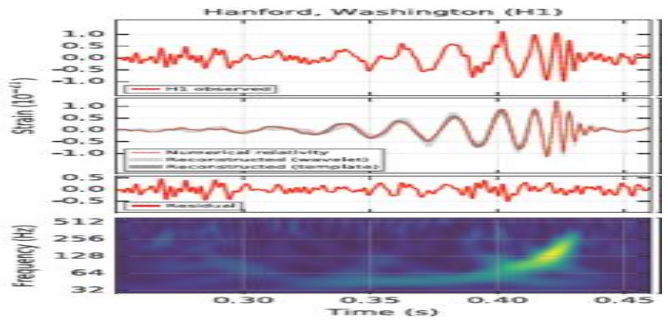

引力波

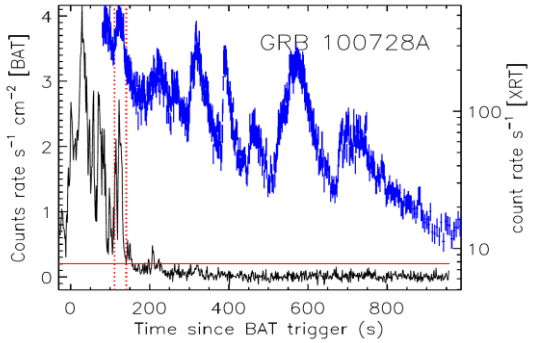

伽马暴和X射线耀发

当今多信使天文、极端条件天体物理研究的最佳对象！

发展暂现源的X射线偏振探测技术，为研究伽马暴辐射机制和新生天体性质及其极早期演化服务。

偏振、光变、能谱、成像是电磁辐射测量四个维度

GRB X射线偏振观测技术难点

- 成熟的X射线偏振探测技术：掠射聚焦、窄视场
- 目标对象：稳定X射线源，如Crab，Vela，磁星等
- 典型在轨项目：IXPE卫星

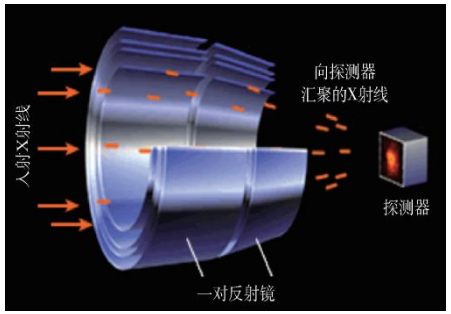

《物理》2021年第8期

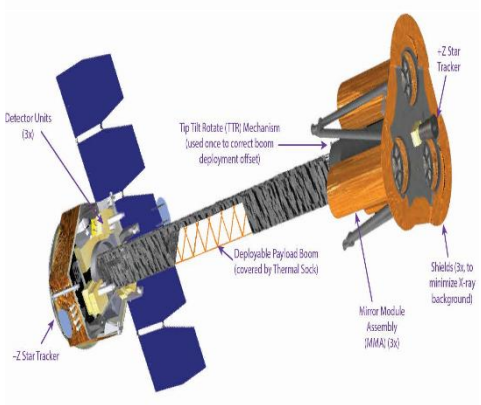

任务和挑战：

- 任 务——宽视场X射线暂现源偏振巡天技术
- 挑 战——暂现源积分时间短，随机性需大视场监测

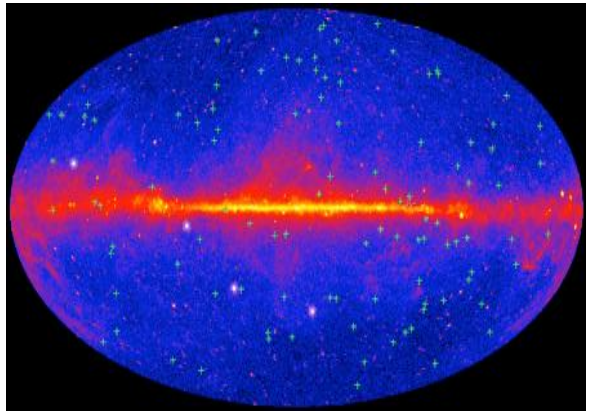

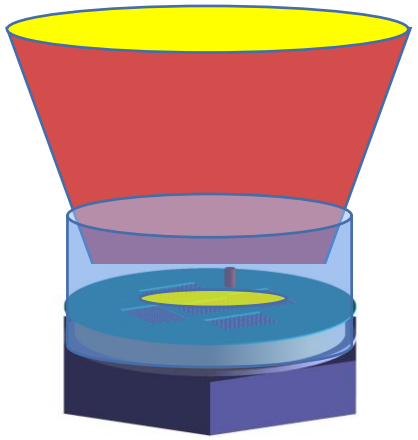

POLAR-2/LPD载荷

➢ 伽马暴偏振探测仪POLAR-2

低能偏振探测器（LPD）

Energy range： 2-10 keV
Detection area： ~ 298 cm2
FoV： ~ 90◦ × 90◦
Energy resolution ： ≤ 20 % @ 5.9 keV
MDP： ~ 10.6% @GRB210619B

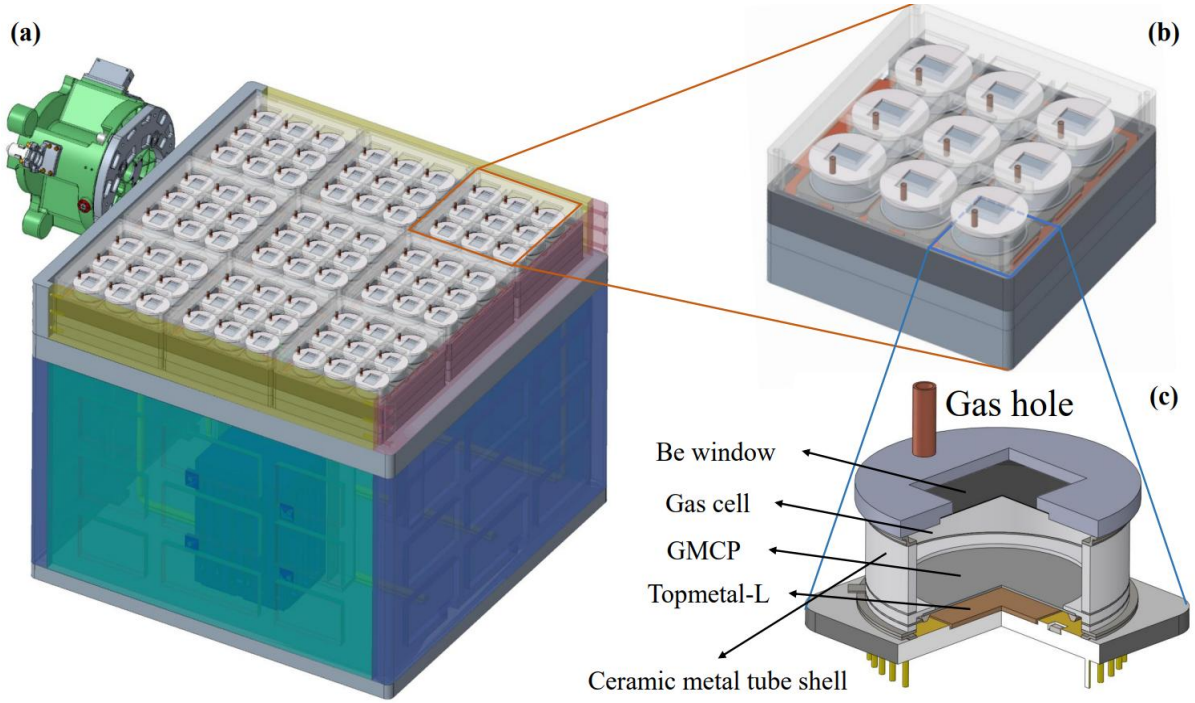

大视场、大面积、阵列化

Z Feng, H Liu et al.*, APJ, 2023

LPD in orbit simulation

- Chinese space station orbit

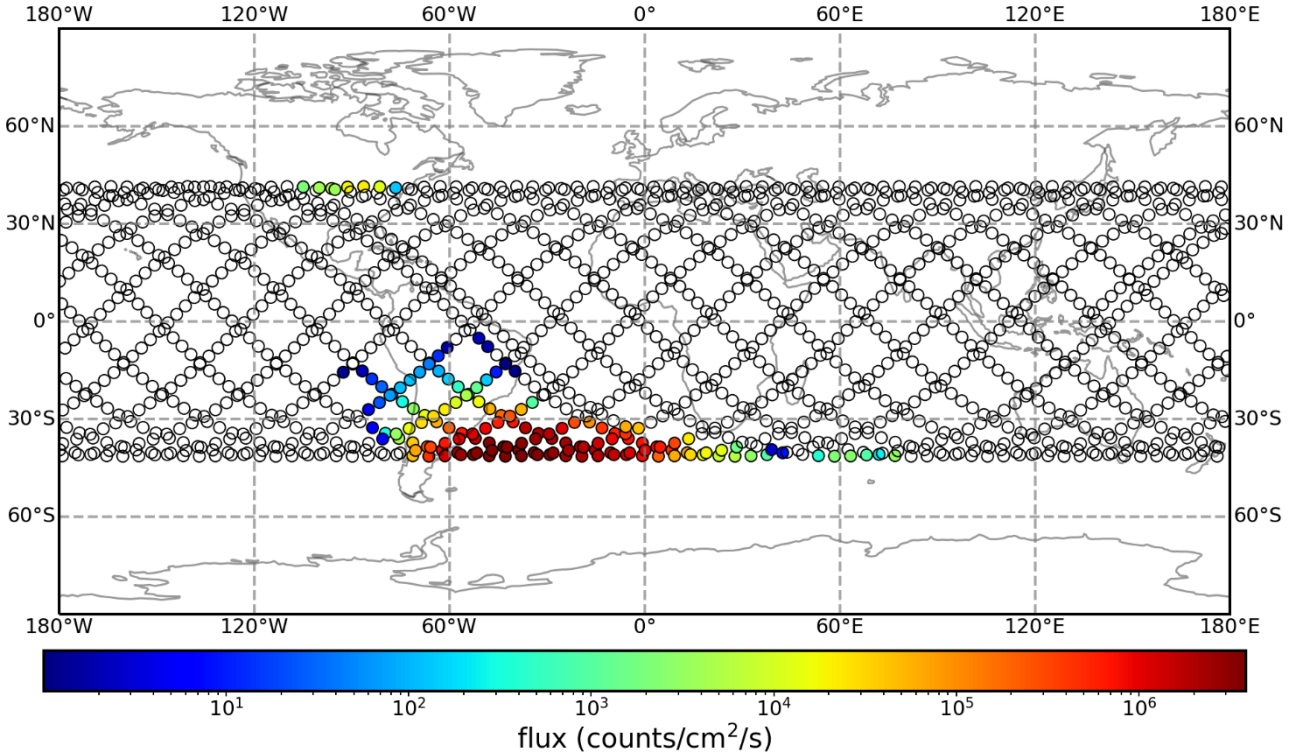

The projection of LPD orbit on Earth in 1 day

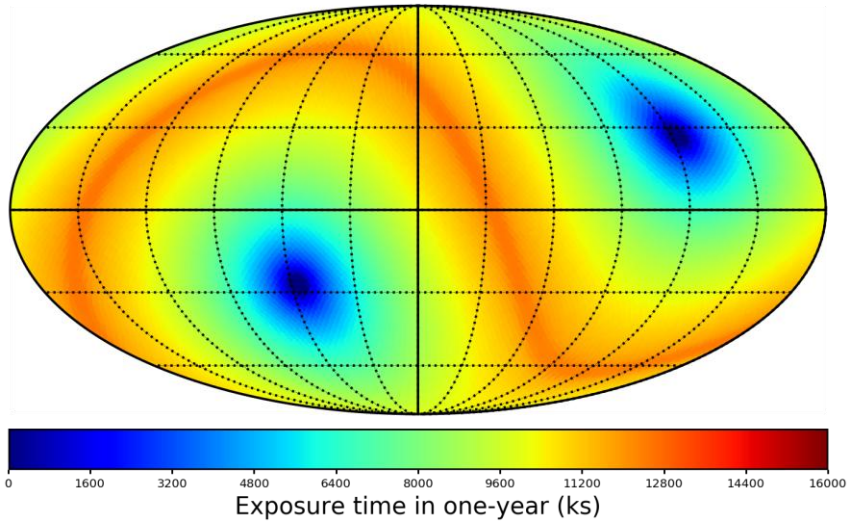

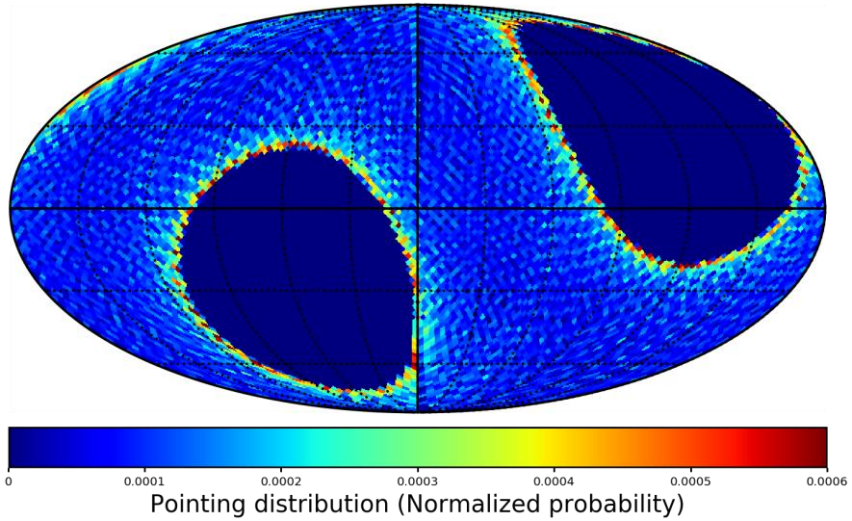

Polarization Statistics

➢ Statistical distribution of MDP of LPD in 5 years

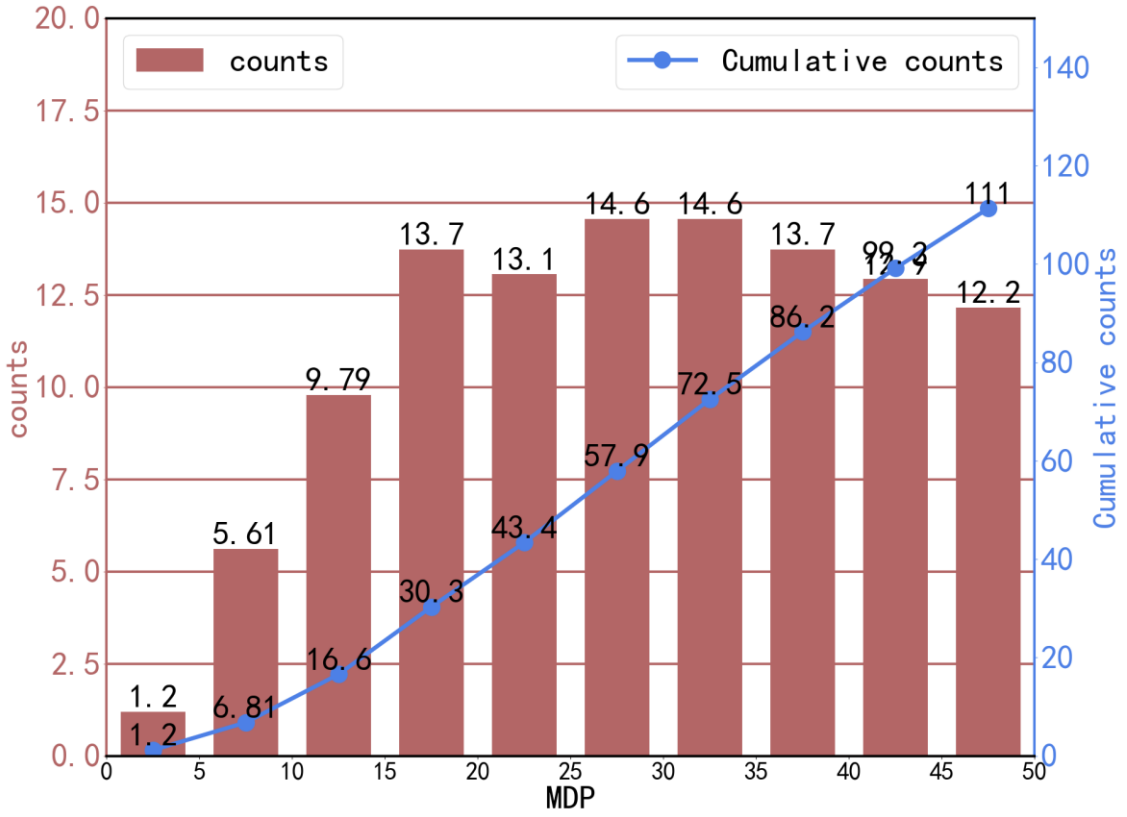

➢ Statistical distribution of PD
(Toma et al. 2009， Lan et al. 2021)

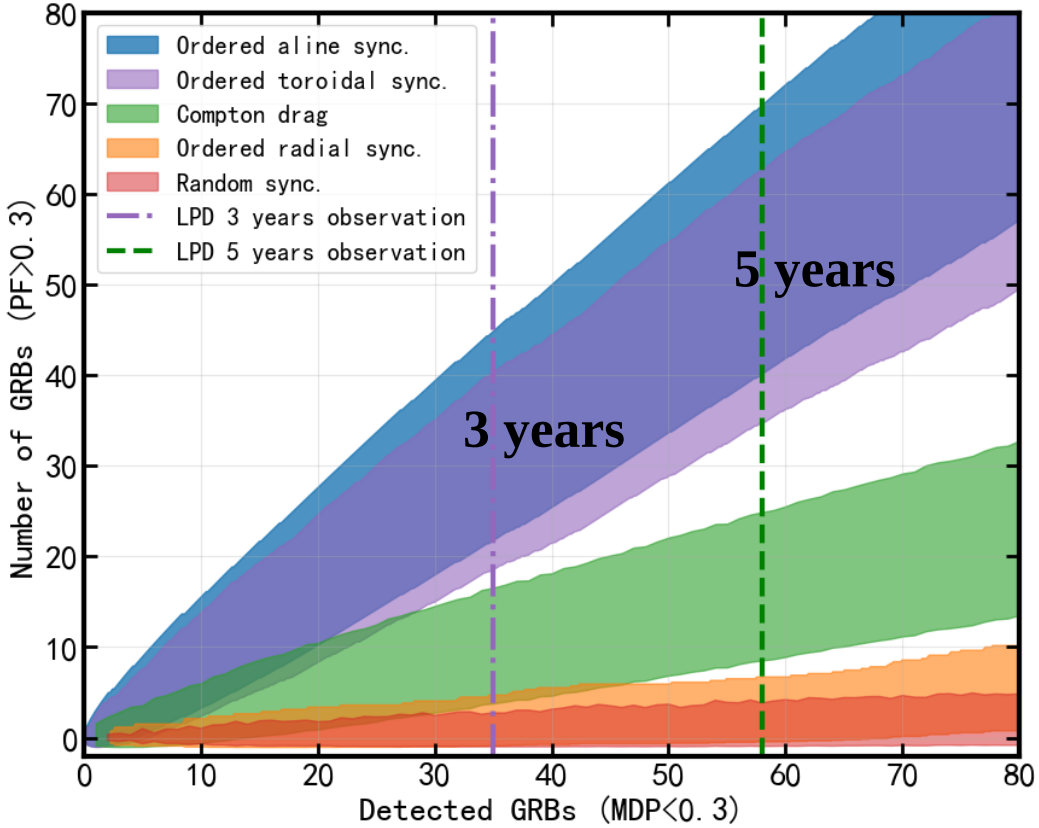

Z Feng, H Liu et al.*, APJ, 2024

The radiation mechanism of GRBs could be determined after 5 years of observations.

X射线偏振探测原理

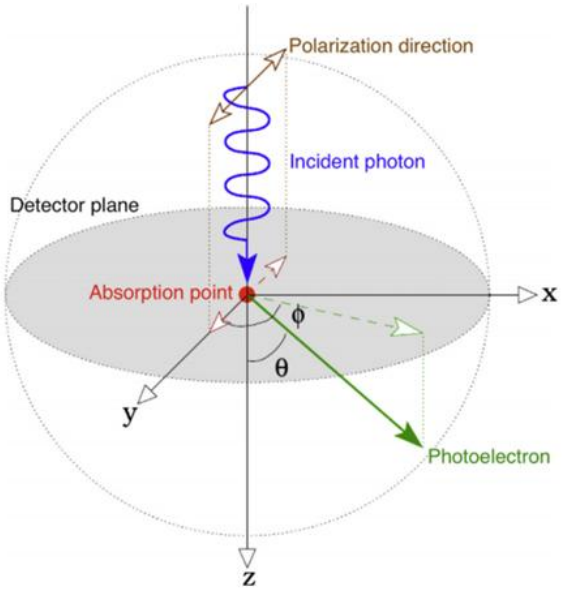

- 光电效应占主导作用
- 在X-Y平面上投影为 $cos^2\emptyset$
- 像素读出，二维成像
- 精确重建光电子出射方向

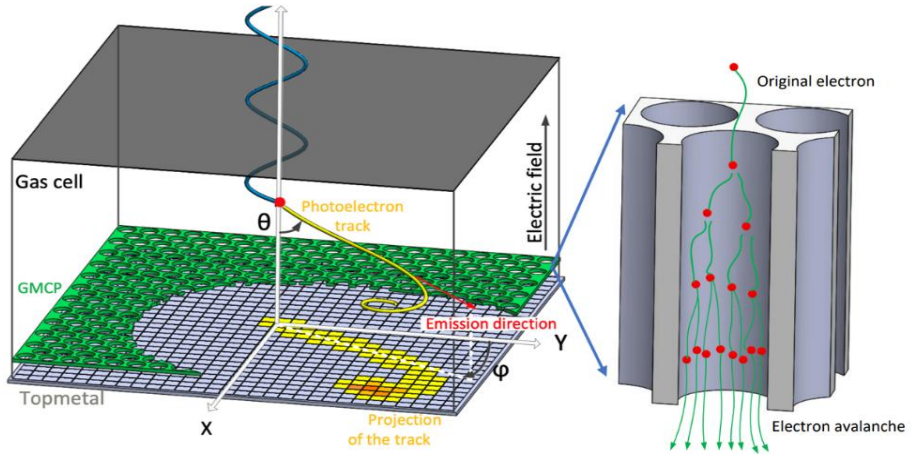

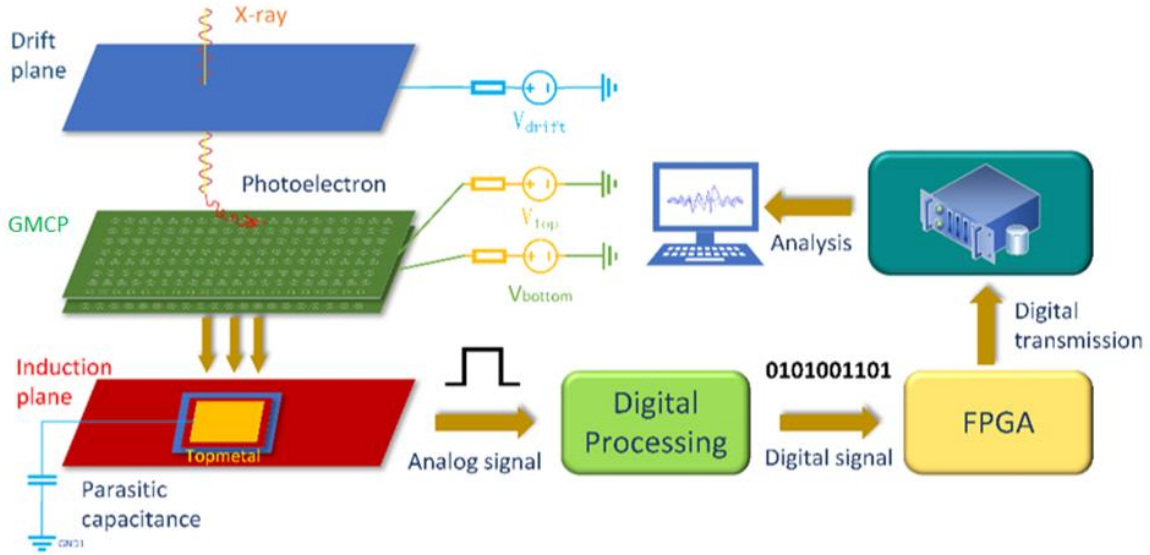

CXPD立方星飞行验证

Cosmic X-ray Polarimeter Detection (CXPD) CubeSat

* Validation of soft X-ray polarization detection technology
* Spatial background measurement
* Standard X-ray source polarization measurement

Size： $96 * 96 * 108\ mm^3$
Mass：~900 g
Power consumption： <5 W

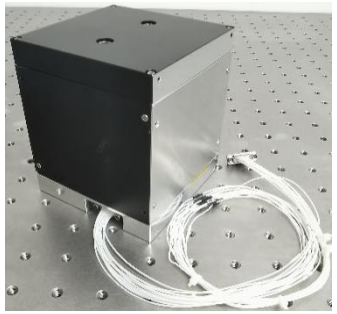

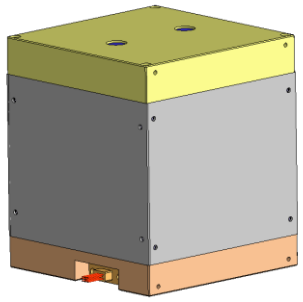

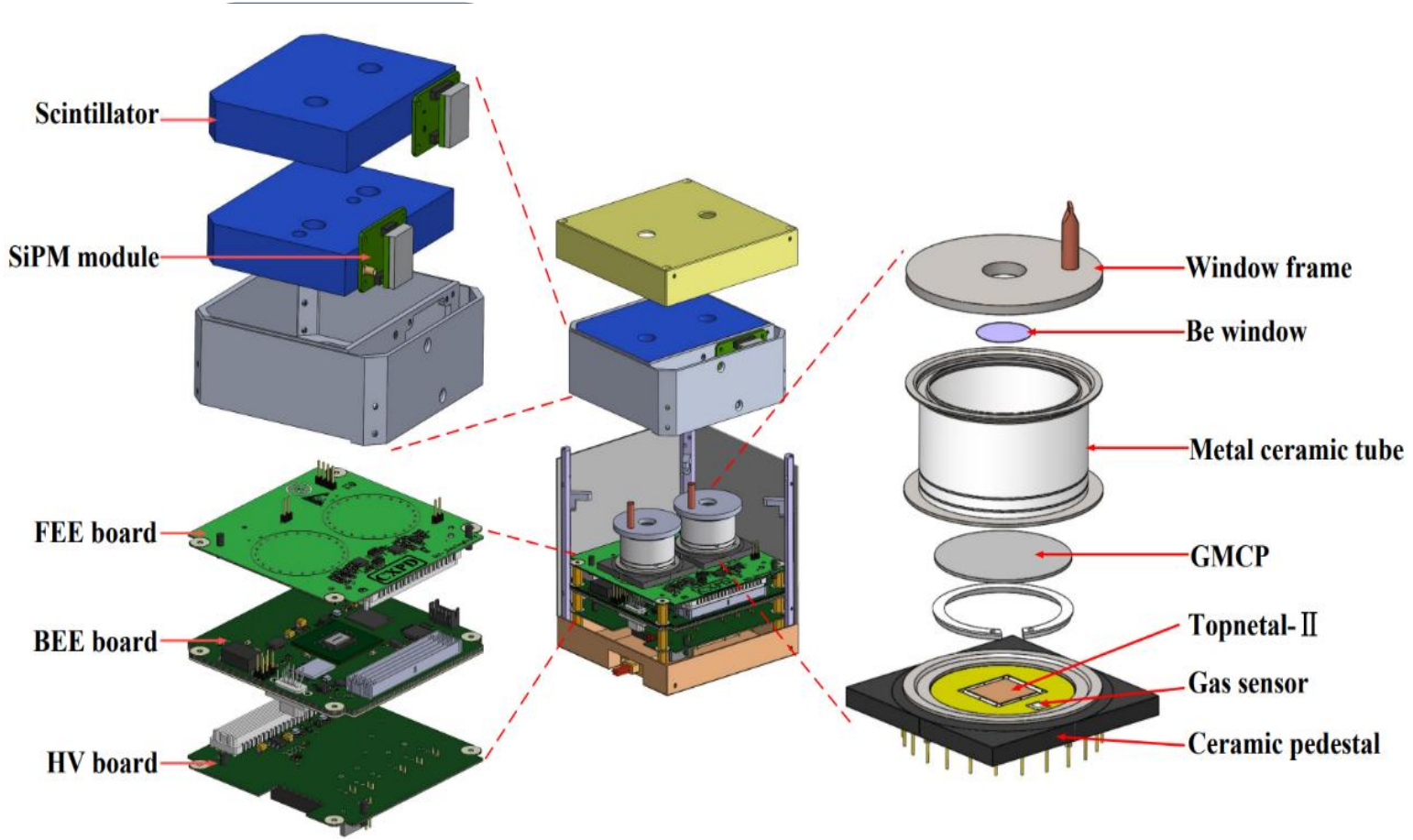

CXPD立方星结构

CXPD有效载荷系统组成和
各功能模块划分

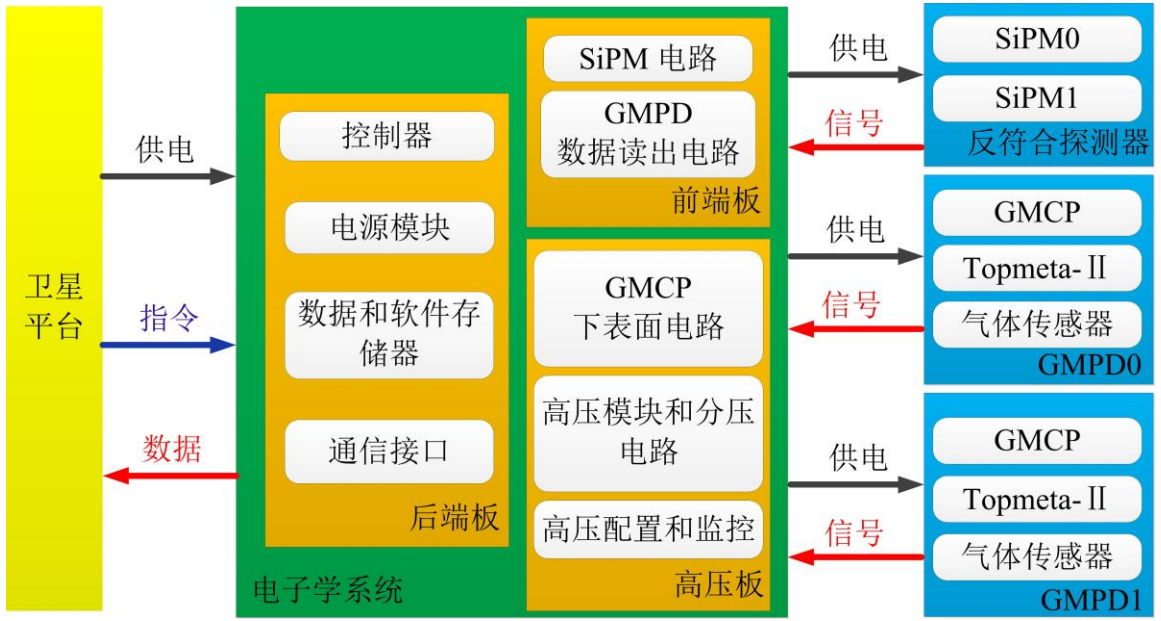

CXPD 记录的数据

Component	Data types			
SiPM data	SiPM trigger time			
GMCP data	GMCP time	GMCP ADC value		
Topmetal data	Topmetal time	Pixel address value	Pixel ADC value	
Monitoring data	HV voltage value	HV current value	GMPD temperature value	GMPD pressure value

H Wang et al., Nucl. Sci. Tech, 2023, Z Fan, H Liu et al., IEEE Trans, 2023*

气体电子倍增器 GEM

- 实现高线性动态范围的关键—气体电子倍增器件

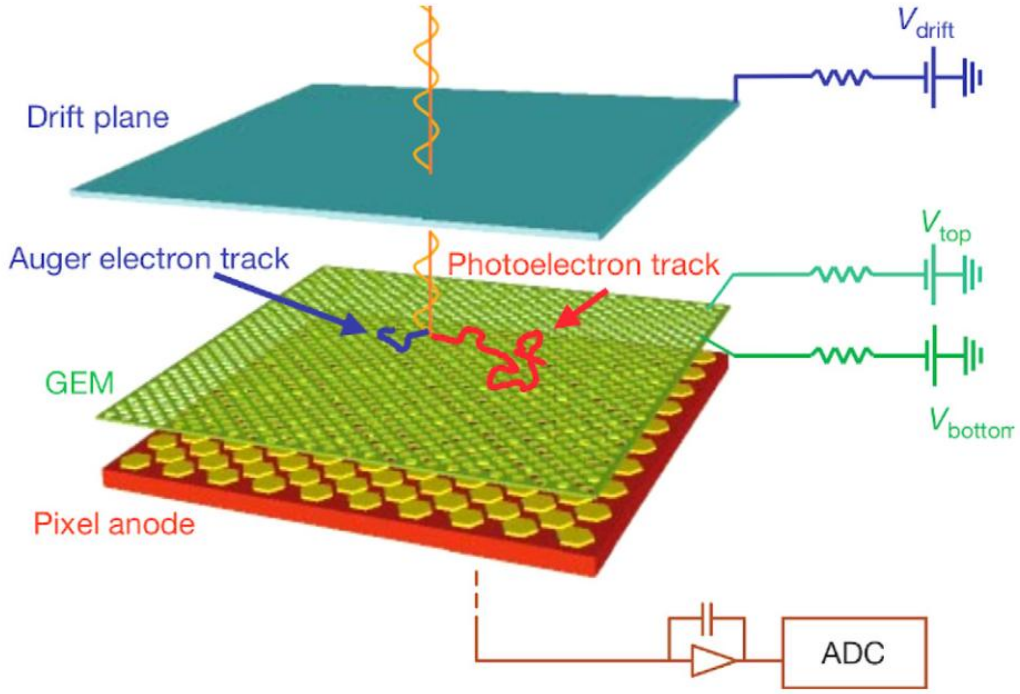

IXPE卫星搭载的GPD探测器
增益随X射线流量的变化

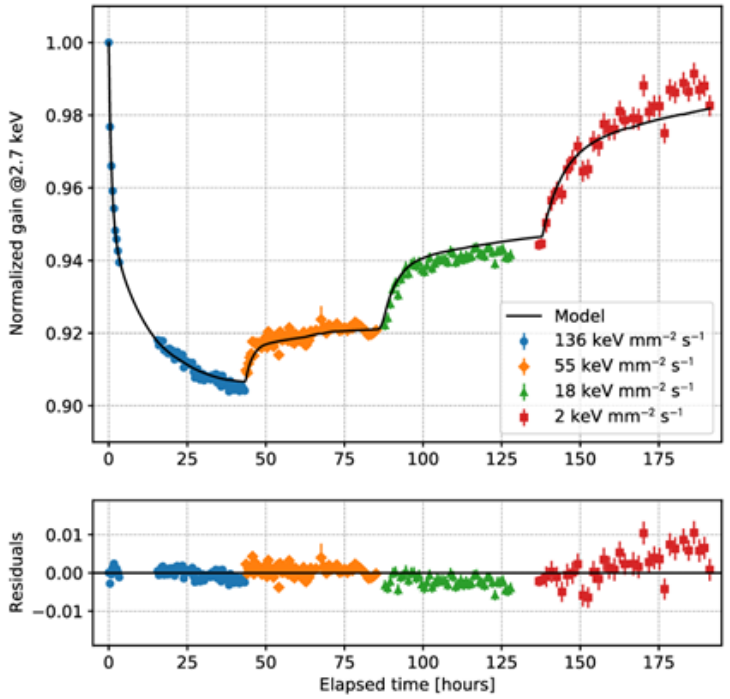

原因：电荷累积在GEM孔内

方案：阻性材料，释放电荷

Baldini, L. et al., Astroparticle Physics, 2021

Gas Microchannel Plate (GMCP)

气体电子倍增微通道板（GMCP）

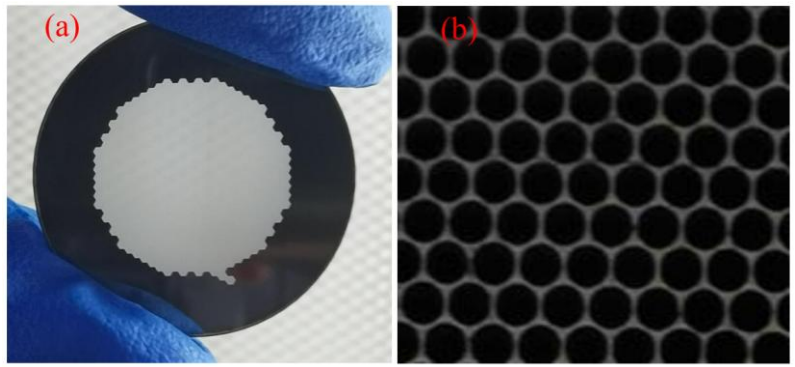

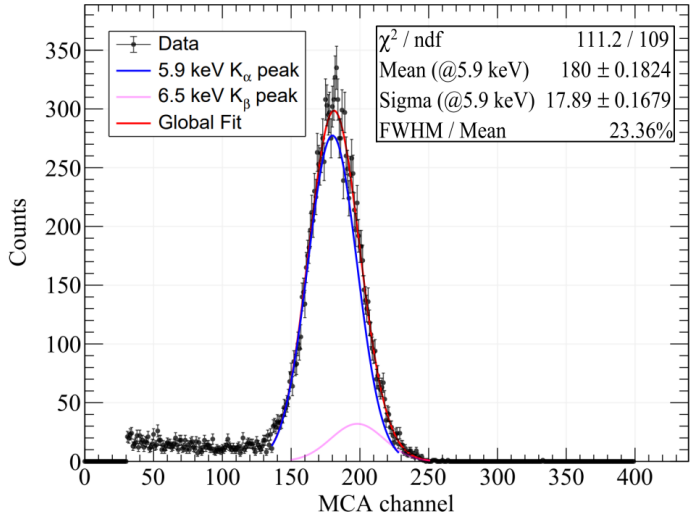

^{55}Fe X-ray spectrum

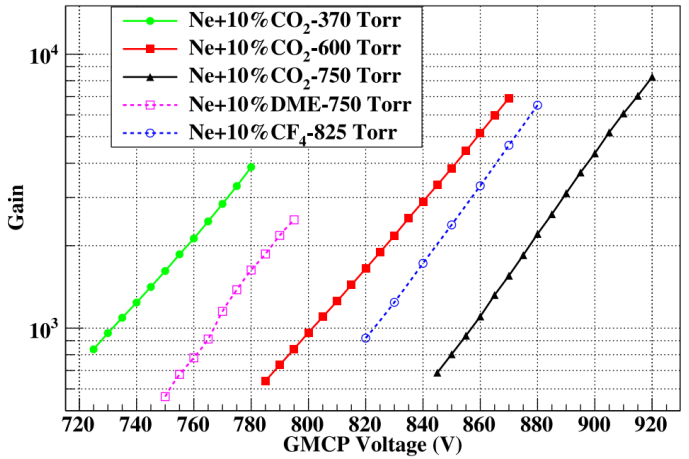

增益与GMCP电极间施加电压的关系

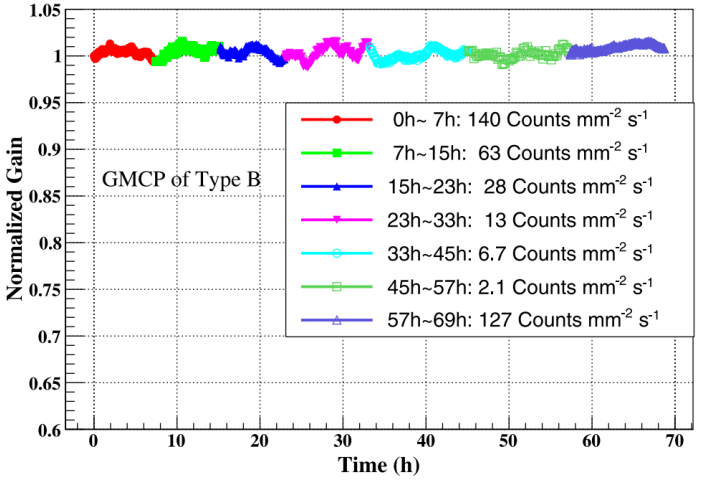

计数率对GMCP增益的影响

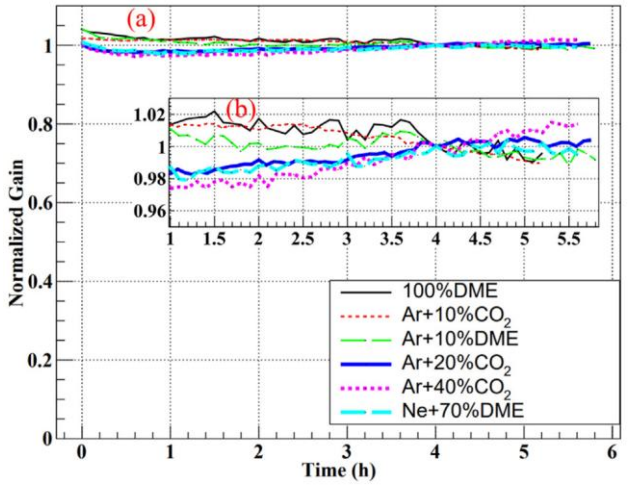

GMCP相对增益随着工作时间的变化

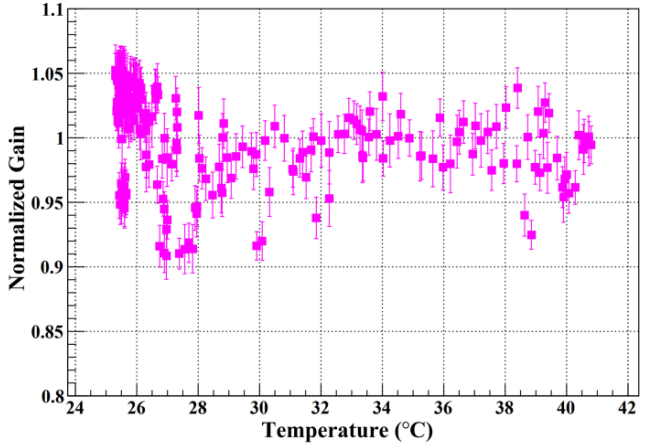

温度的对GMCP增益的影响

H Feng, H Liu et al., Nucl. Instrum. Meth. A , 2023*

Topmetal 芯片

CXPD 采用的像素芯片： Topmetal-II

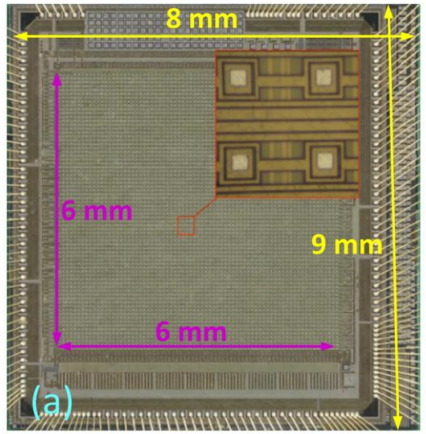

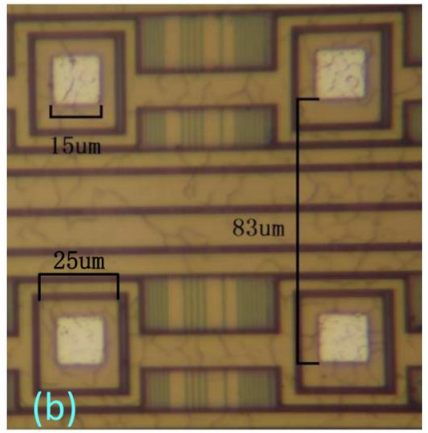

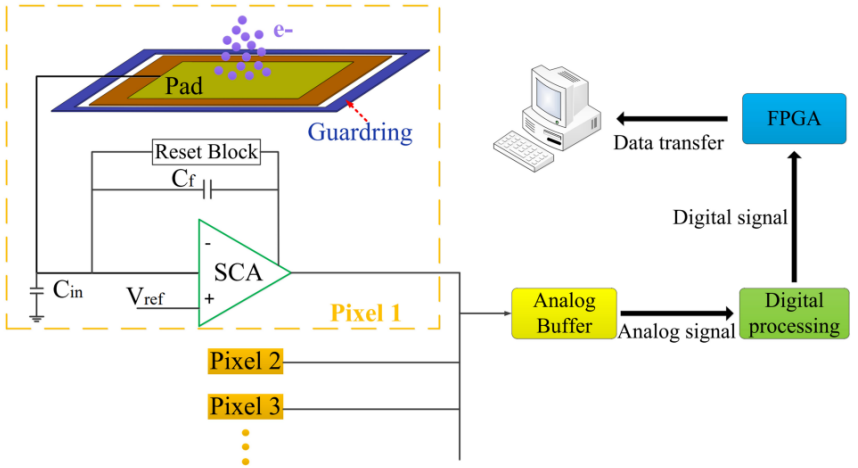

	Topmetal-II⁻	Topmetal-M1/M2	Topmetal-L
Chip Size /mm²	6 × 6	18 × 23	17 × 24
Pixel Array	72 × 72	400 × 512	356 × 512
Pixel Size /um²	83 × 83	45 × 45	45 × 45
Pixel Electrode / um²	15 × 15	10 × 20	26 × 26
ENC	~ 13.4e-	~ 15.4e-	~ 20.0e-
Power Consumption	~ 1W @3.3V	~ 4.3W @3.3V	**~ 0.8W @3.3V**
Clock	40MHz	5MHz	20MHz
Frame Rate	2.5ms	2.4ms	0.37ms @Sentinel Readout
Readout Mode	Rolling Shutter	Rolling Shutter	Rolling Shutter **/Sentinel Readout**
Readout Channel	1	16	1

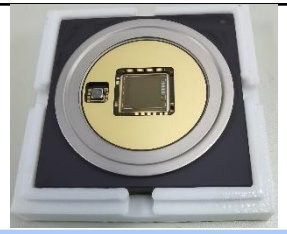

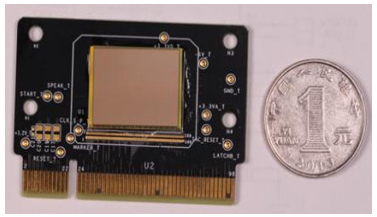

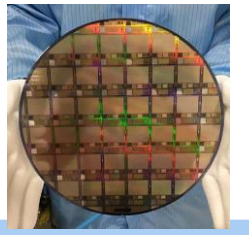

Z Li,..,H Liu et al., Nucl. Instrum. Meth. A , 2021*

Topmetal 芯片读出电路

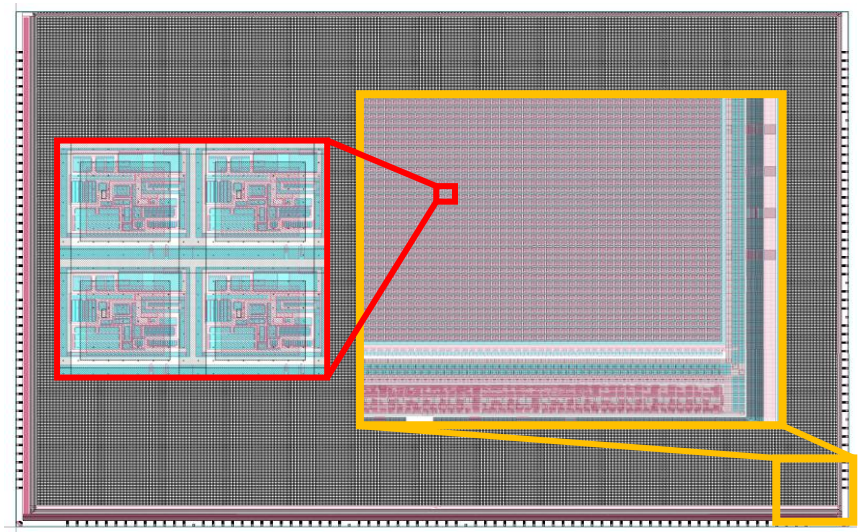

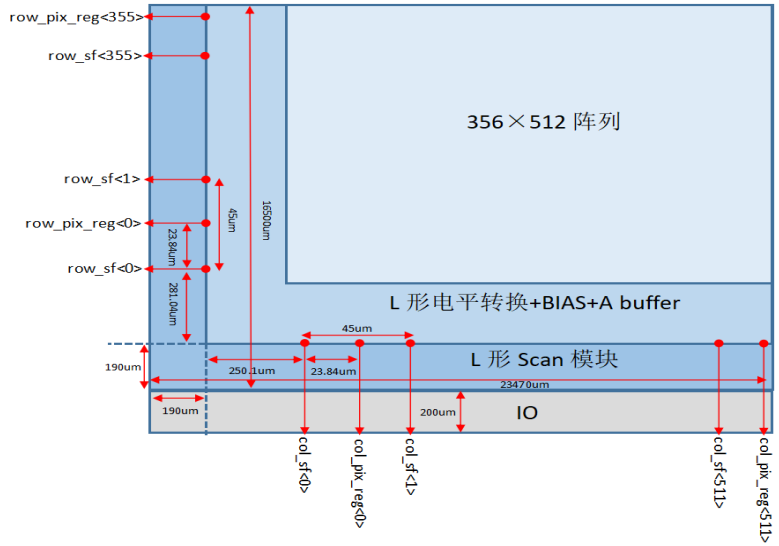

Topmetal-L layout structure.

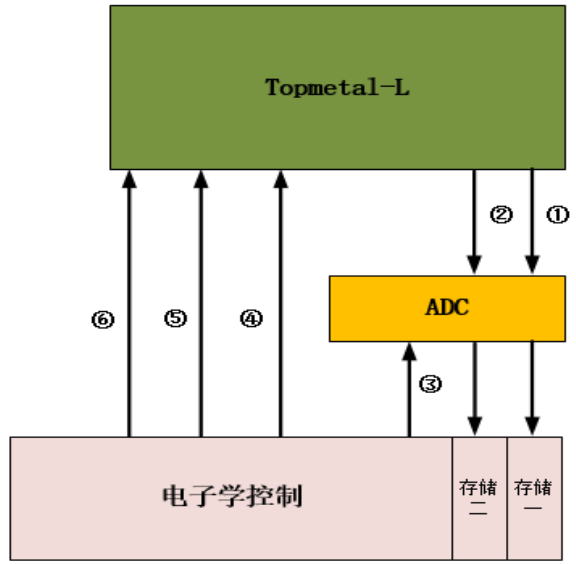

Data communication instructions.

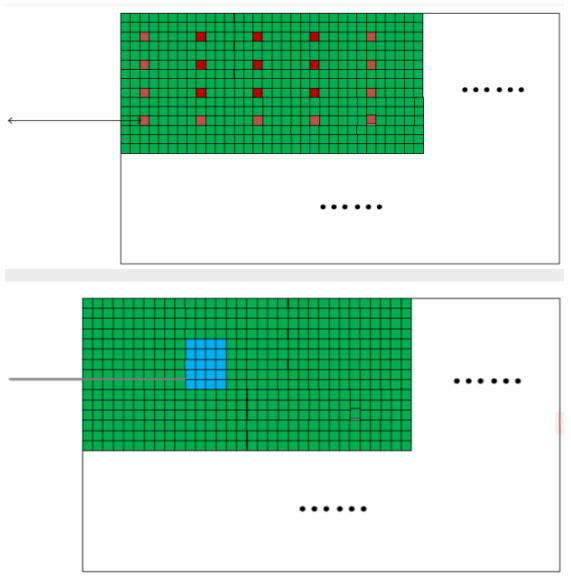

Sentry scanning and area scanning.

In the readout section of the Topmetal-L chip, a novel readout scheme called the **Sentinel readout scheme** is adopted.

X-ray 光电子径迹

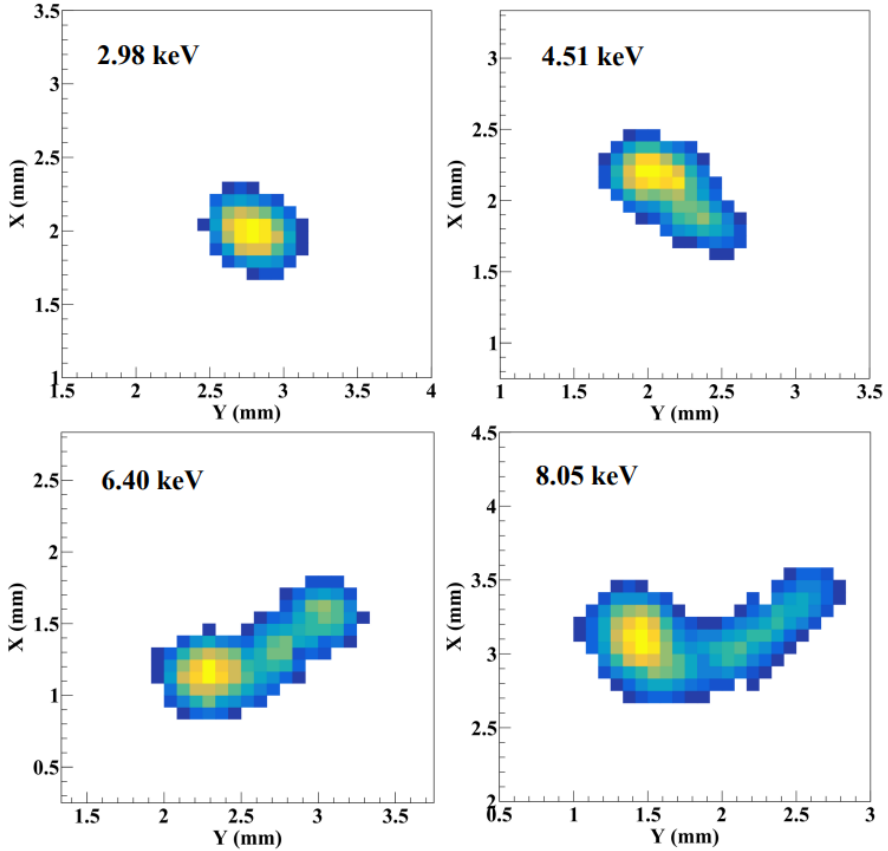

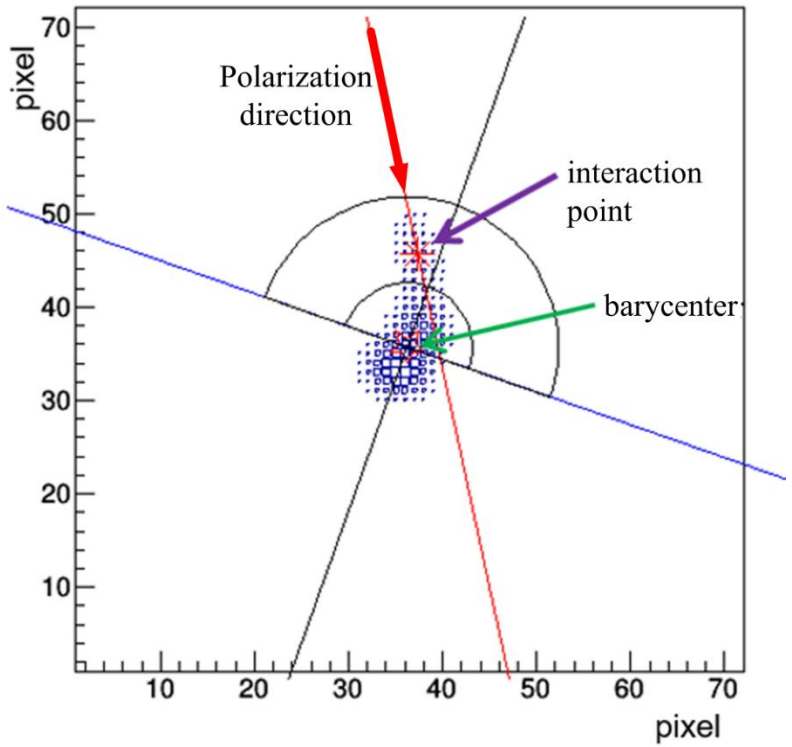

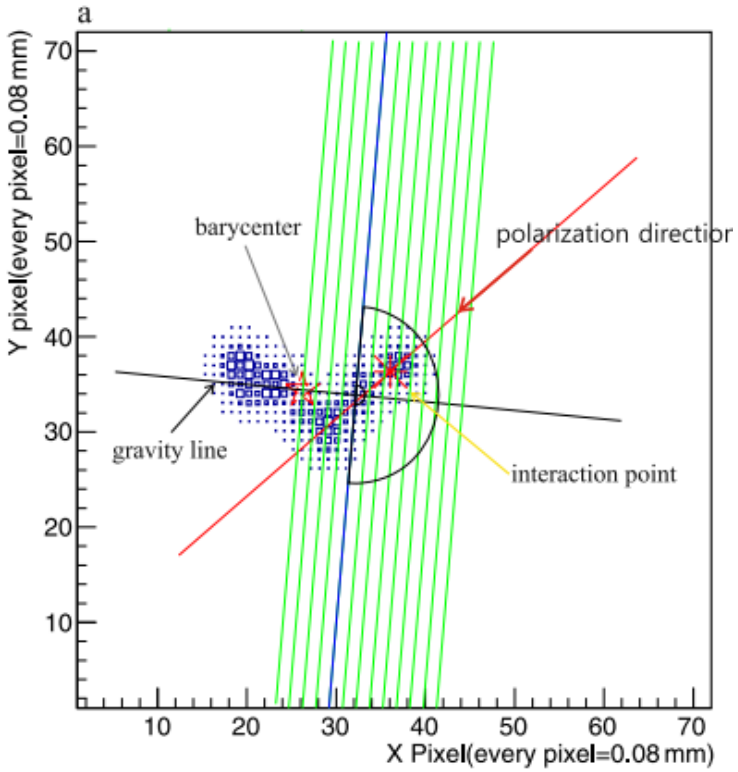

X Huang, H Liu et al., Nucl. Sci. Tech, 2021*

GMCP 下表面读出电路

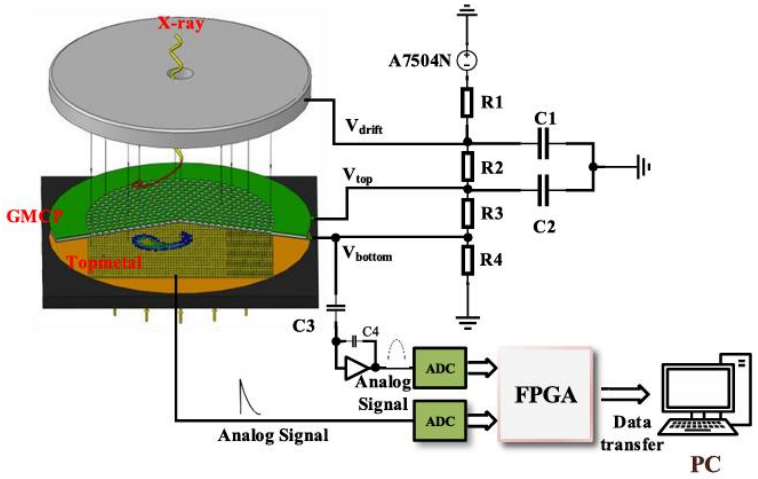

Schematic of the GMPD experimental system.

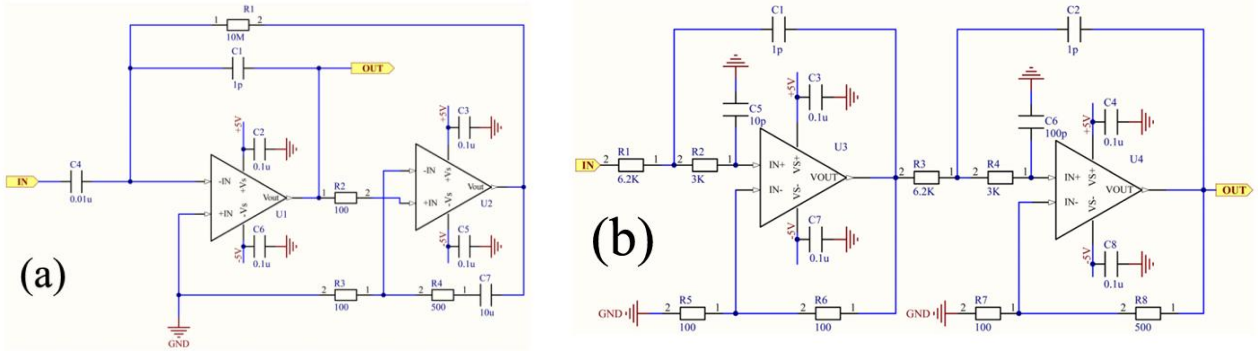

GMCP's bottom amplifier circuit. (a) CSA. (b) Filter shaper.

- Improve the time resolution and energy resolution.

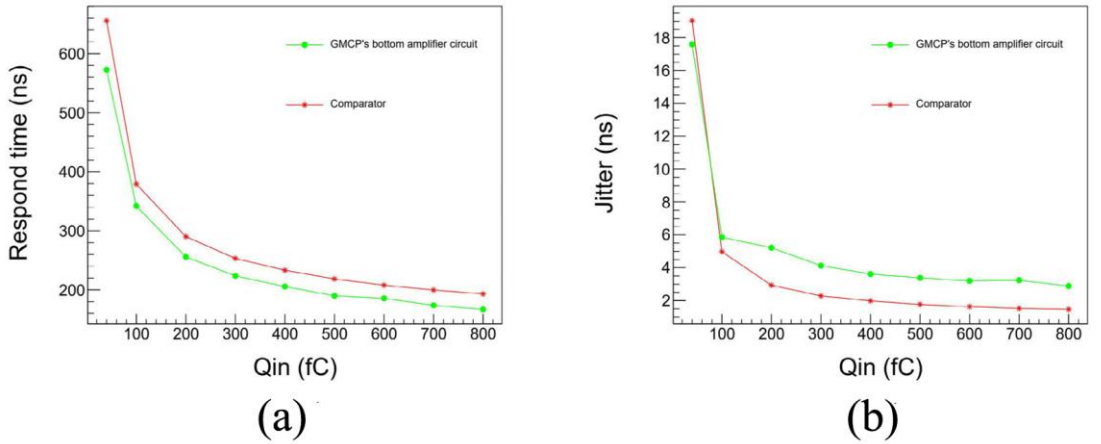

Time performance of the GMCP's bottom amplifier circuit. (a) Time walk. (b) Time accuracy.

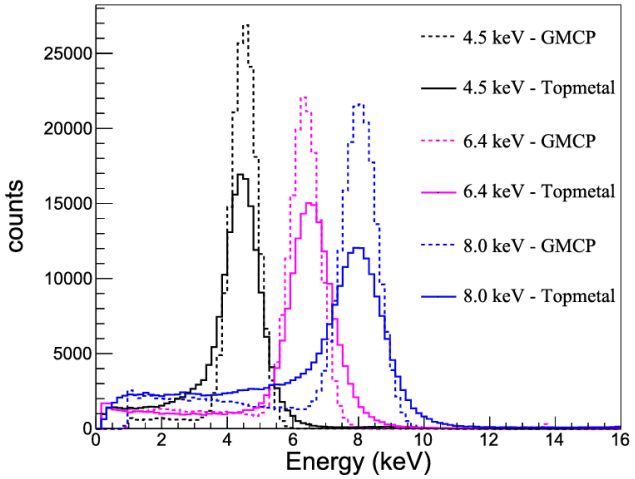

Energy spectrum of GMCP and Topmetal-II after events matching.

Z Fan, H Liu et al., IEEE Trans, 2023*

气体探测器封装

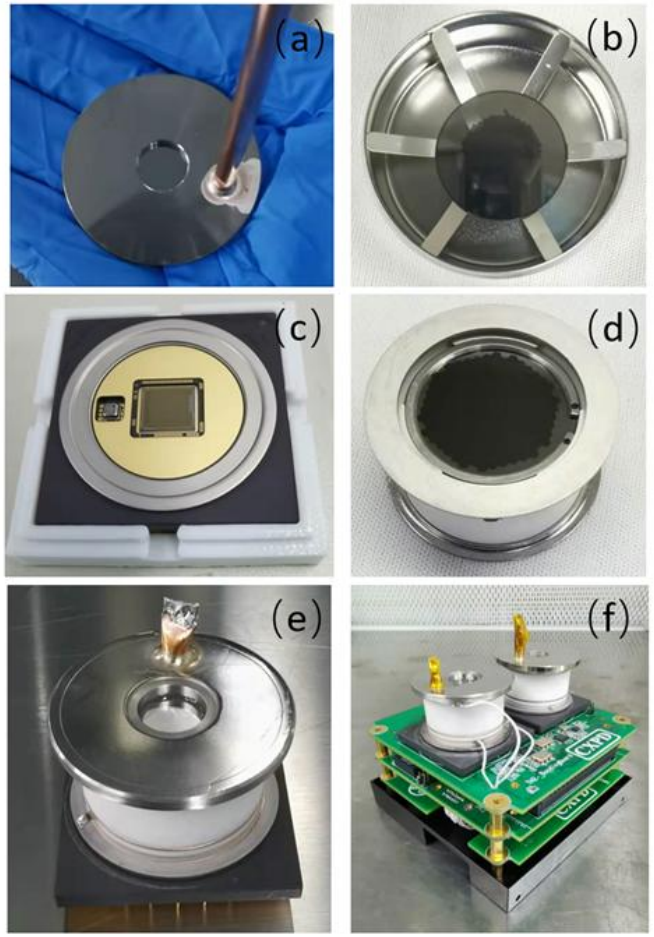

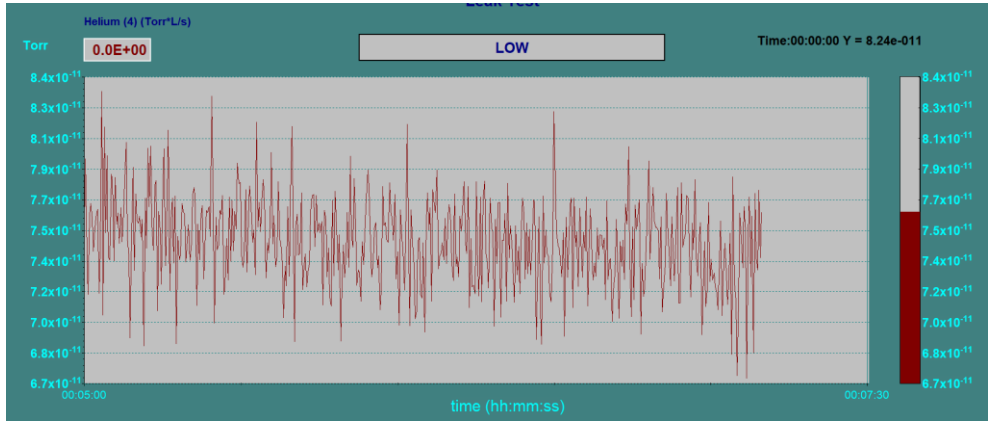

Leakage rate： 7.6^{-11} Torr*L/s

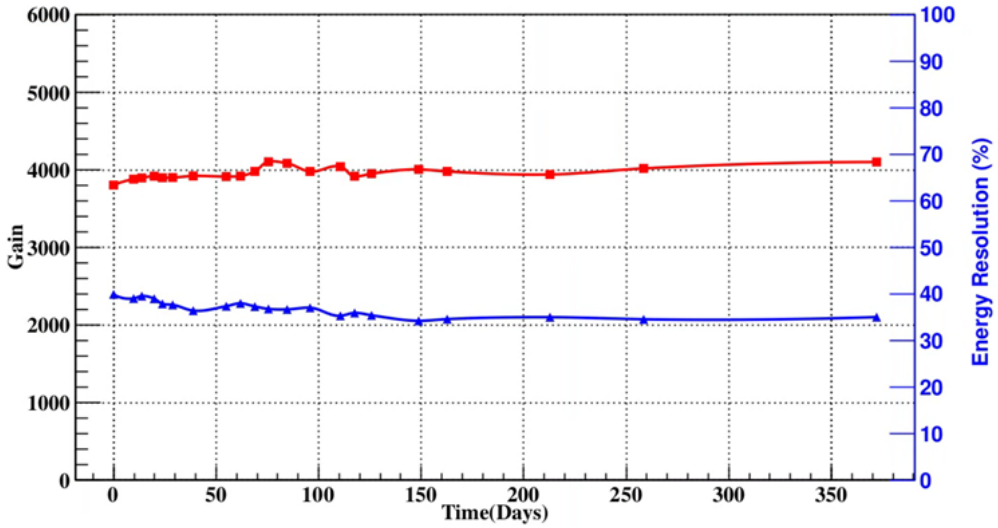

长期稳定性测量

H Feng, H Liu et al., Nucl. Sci. Tech, 2023*

X-ray 标定平台

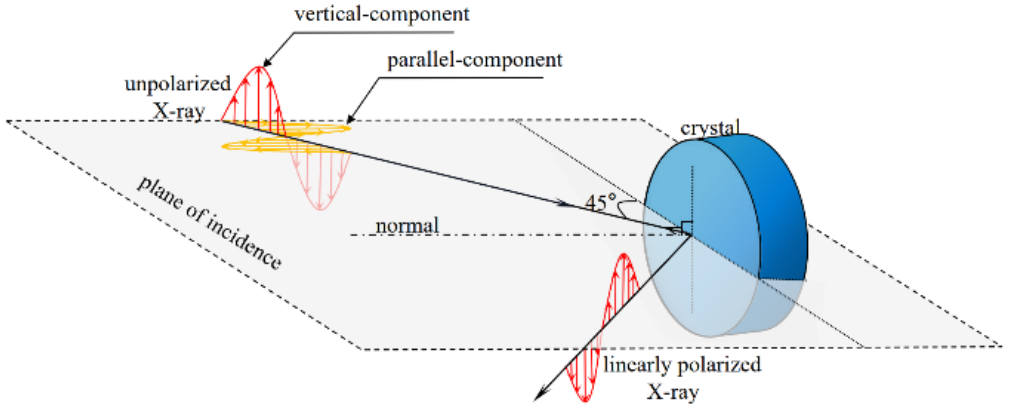
vertical-component
parallel-component
unpolarized
X-ray
crystal
45°
normal
plane of incidence
linearly polarized
X-ray

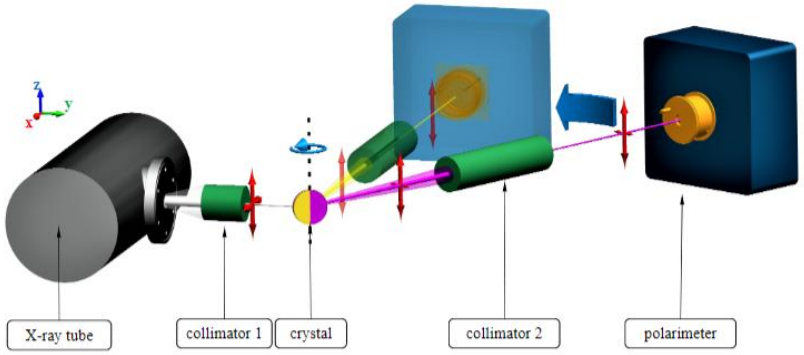
X-ray tube
collimator 1
crystal
collimator 2
polarimeter

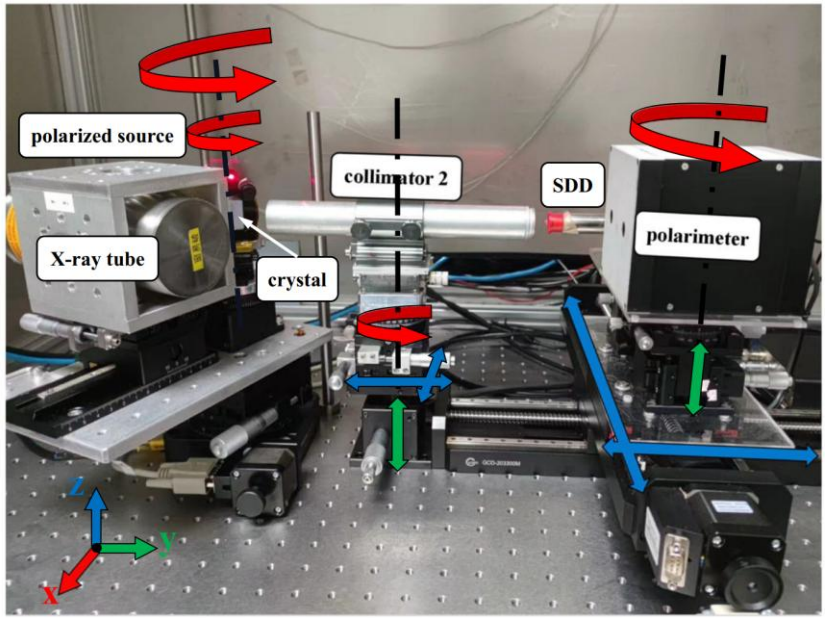
polarized source
collimator 2
SDD
polarimeter
X-ray tube
crystal
z
y
x

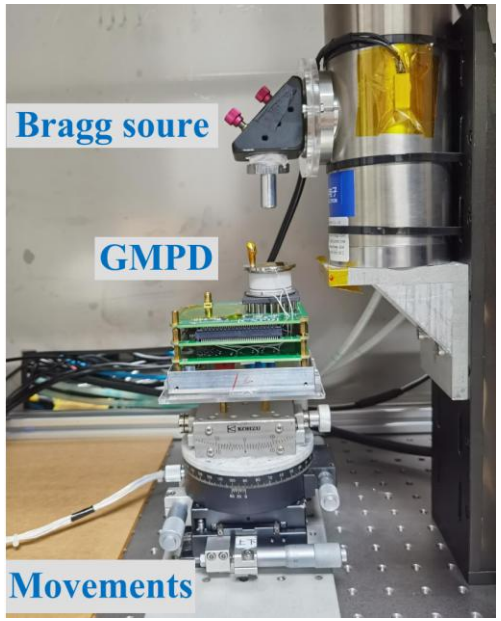
Bragg soure
GMPD
Movements

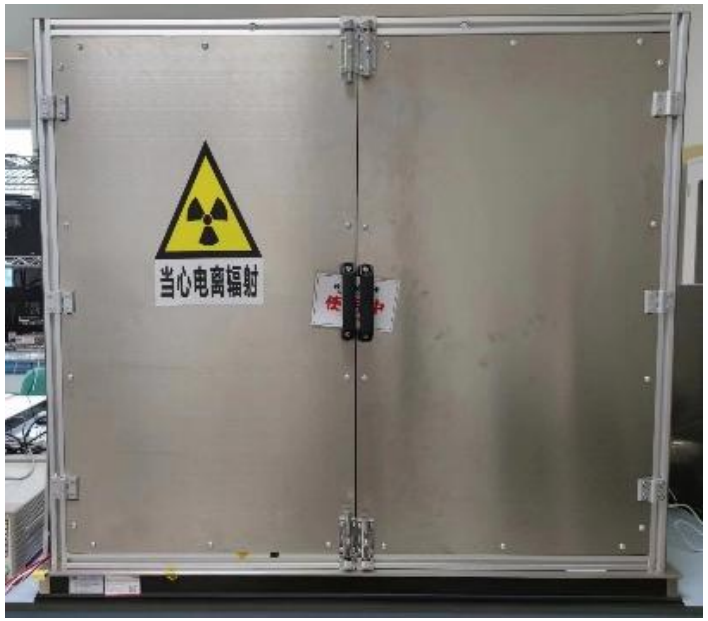
当心电离辐射

X-ray polarized calibration platform

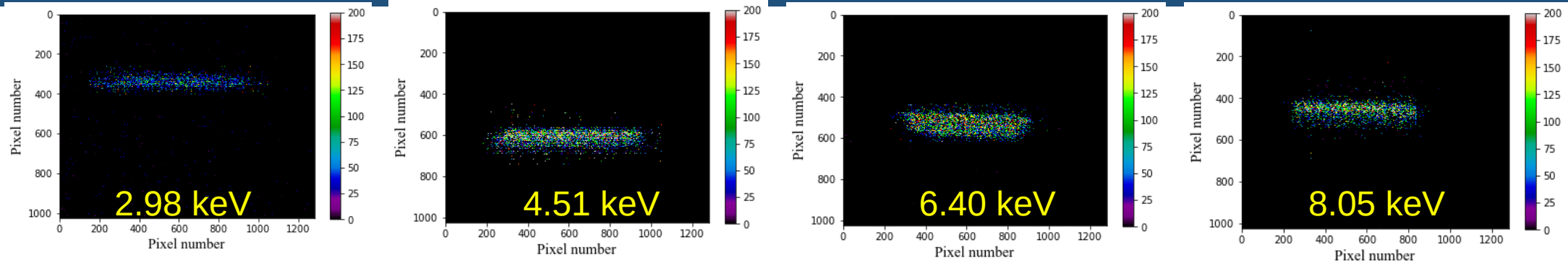

Image with the CCD imager of the photons generated with the polarized source.

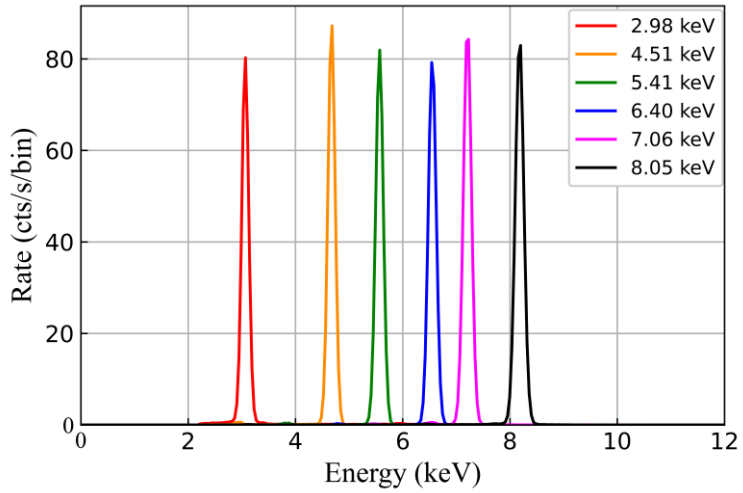

Spectrum of the polarized source.

Y Xie, H Liu* et al., EXP ASTRON, 2023

TABLE II. Configurations and performance list of 8.05 keV linear polarized sources. The polarization degree is calculated using Eq. (3).

Energy(keV)	2.98	4.51	5.40	6.40	7.06	8.05
Crystal	Si(111)	Si(220)	Si(311)	Si(400)	Si(331)	Si(224)
Incident radiation	Ag L_α	Ti K_α	Cr K_α	Fe K_α	Fe K_β	Cu K_α
Diffraction angle(deg)	41.6	45.8	44.5	45.5	44.9	44.1
Rate(cts/s)	207.52	375.49	370.49	375.8	426.77	439.25
Proportion of monochromatic light[a](%)	93.04	97.91	98.31	98.64	97.40	97.32
FWHM(eV)	139.38	146.69	149.39	142.42	158.62	159.73
X-ray tube settings	8.0 kV, 0.49 mA	6.5 kV, 0.19 mA	7.0 kV, 0.19 mA	8.0 kV, 0.31 mA	9.8 kV, 0.44 mA	9.5 kV, 0.58 mA
Polarization(%)	97.4	99.8	99.9	99.8	99.9	99.8

[a] The proportion of monochromatic light is defined as the ratio of the number of photons falling within three times the sigma of the target peak centre value to the total photons.

TABLE III. Configurations and performance list of 8.05 keV partially polarized sources. The copper Kα characteristic line diffracted by silicon crystal to generate beams with different degrees of polarization. The polarization degree is calculated using Eq. (3).

Energy(keV)	8.05	8.05	8.05	8.05	8.05	8.05
Crystal	Si(111)	Si(220)	Si(311)	Si(400)	Si(331)	Si(224)
Incident radiation	Cu K_α	Cu K_α	Cu K_α	Cu K_α	Cu K_α	Cu K_α
Diffraction angle(deg)	14.2	23.7	28.1	34.6	38.2	44.1
Rate(cts/s)	277.75	166.66	224.14	657.92	146.97	555.92
Proportion of monochromatic light[a](%)	92.82	96.84	98.32	98.40	98.36	98.37
FWHM(eV)	193.05	162.63	159.61	159.24	159.11	159.73
X-ray tube settings	9.3 kV, 0.19 mA	9.4 kV, 0.39 mA	10.3 kV, 0.19 mA	11.5 kV, 0.29 mA	10.0 kV, 0.19 mA	10.5 kV, 0.29 mA
Polarization(%)	12.8	37.0	52.6	77.5	89.5	99.8

[a] The proportion of monochromatic light is defined as the ratio of the number of photons falling within three times the sigma of the target peak centre value to the total photons.

Spectral and polarimetric characterization

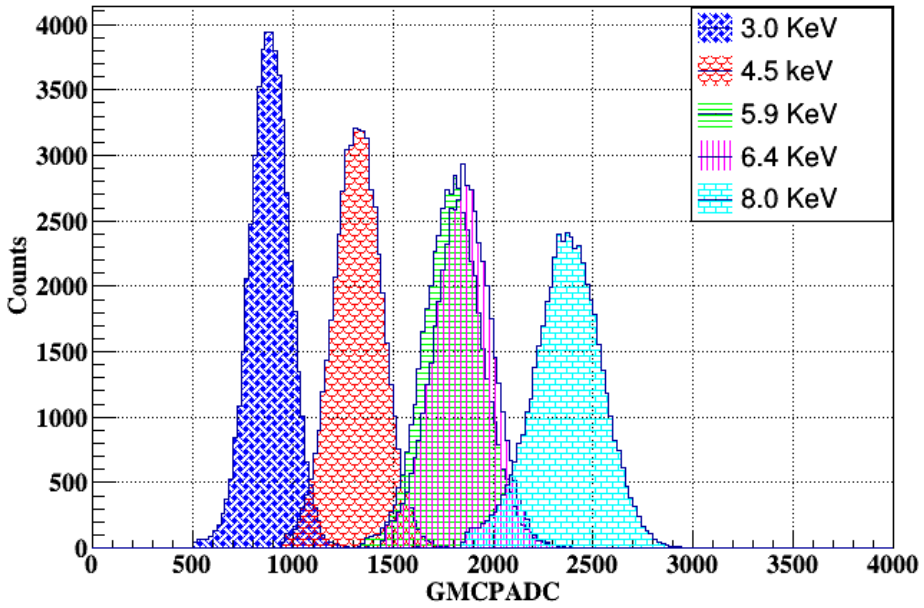

Energy spectra measured with Bragg diffractions.

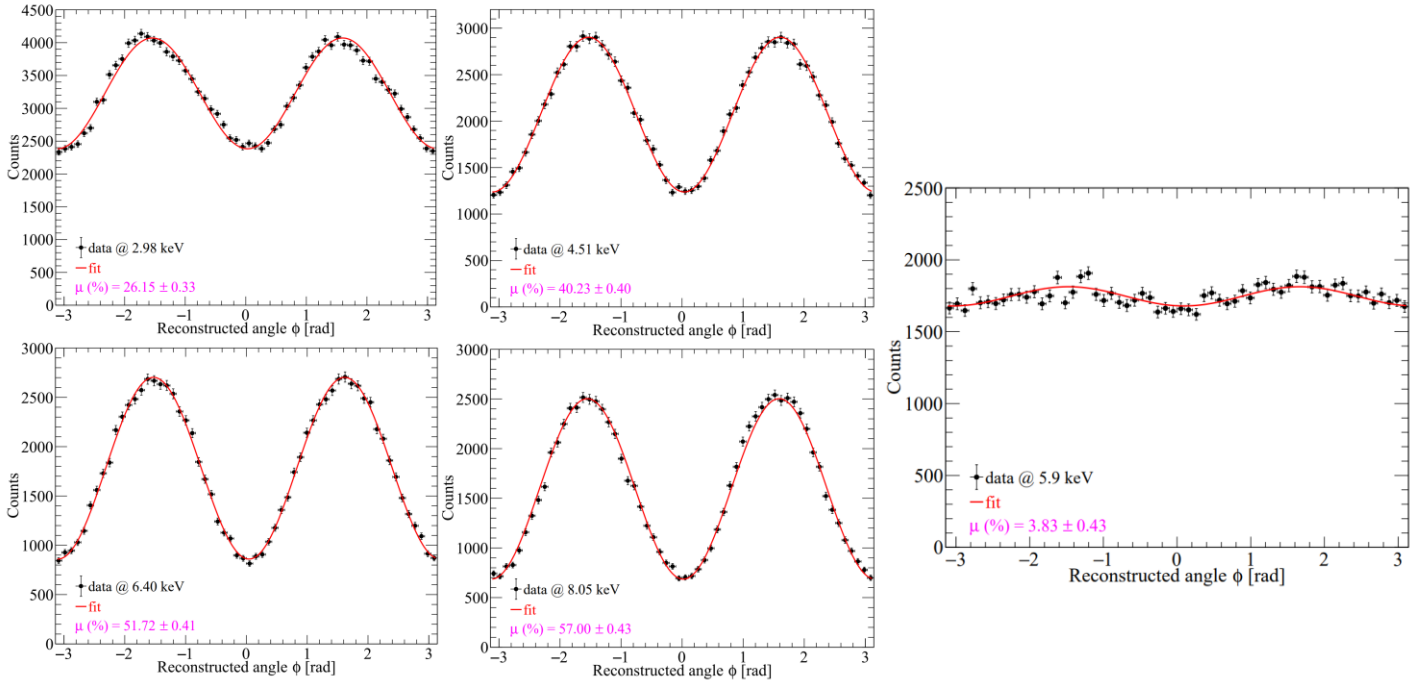

Modulation curves measured with polarized and unpolarized X-ra

Energy (keV)	E_{peak} (ADC)	FWHM (ADC)	FWHM/E_{peak}
2.98	885.5 ± 0.5	230.3 ± 0.9	0.260 ± 0.002
4.51	1323.1 ± 0.6	285.0 ± 1.1	0.215 ± 0.001
6.40	1880.1 ± 0.7	338.9 ± 1.4	0.180 ± 0.001
8.05	2369.6 ± 0.9	190.1 ± 1.7	0.165 ± 0.001

GMPD, 40%He+60%DME, 0.8 atm		
Energy (keV)	μ	$\mu\sqrt{\varepsilon}$
2.98	0.2615 ± 0.0033	0.0753
4.51	0.4023 ± 0.0040	0.0749
6.40	0.5172 ± 0.0041	0.0608
8.05	0.5700 ± 0.0043	0.0486

H Feng, H Liu et al., JINST, 2023*

CXPD 组装

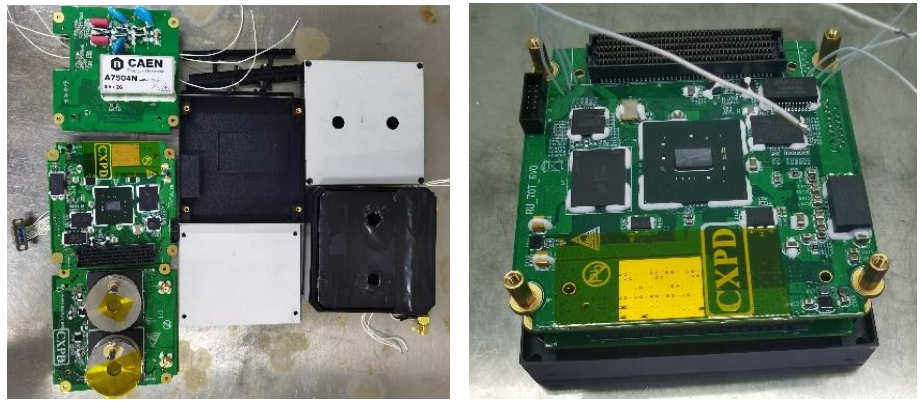

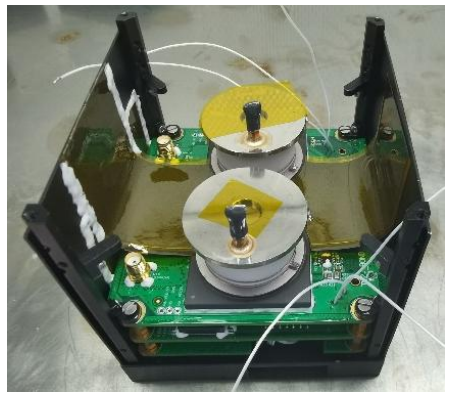

Assembly process of the CubeStar payload

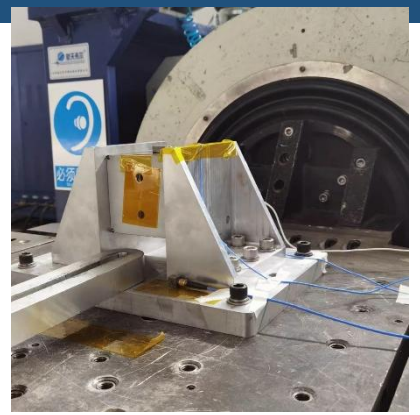

Vibration test

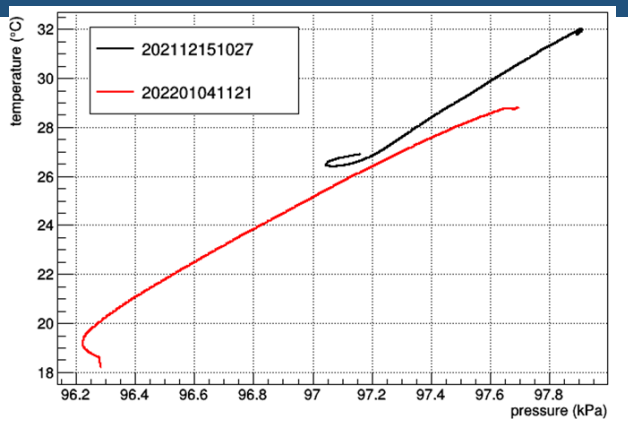

照

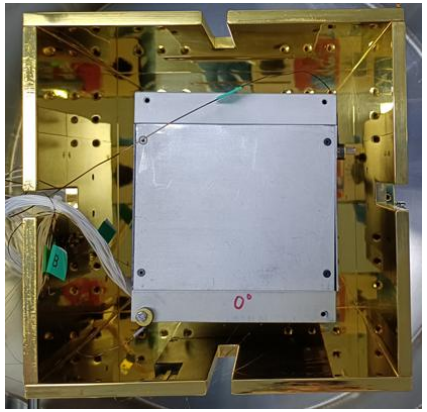

Thermal vacuum test

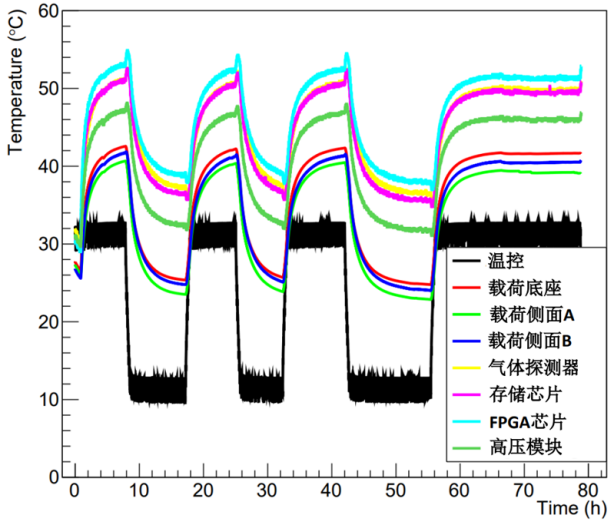

CXPD Collaboration

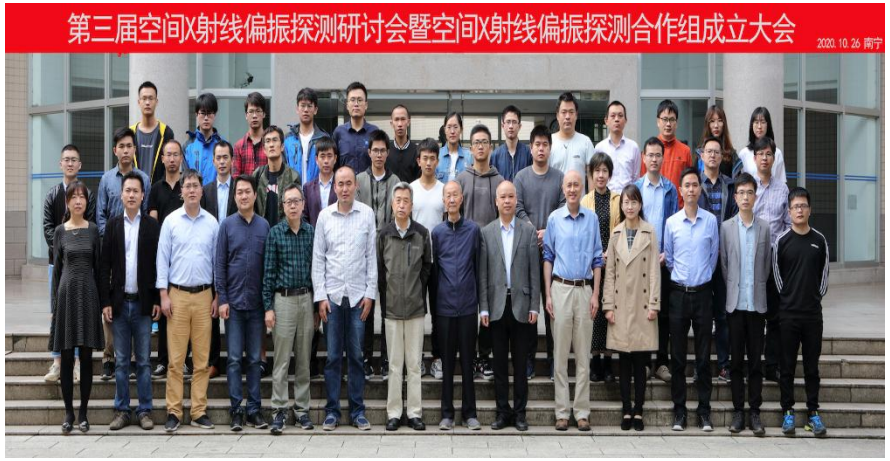

2020.10 第3届，广西大学

2023.8 第5届，广西大学

2019.7.11 第1届CXPD合作组会在航天五院召开

2020.1.5 第2届CXPD合作组会在华中师范大学召开

2022.8 第4届，广西大学

谢 谢!